Iron Availability Within the Leaf Vasculature Determines the Magnitude of Iron Deficiency Responses in Source and Sink Tissues in Arabidopsis

Nga T Nguyen, Mather Khan, Norma Castro-Guerrero, Ju-Chen Chia, Olena Vatamaniuk, Stéphane Mari, Silvia Jurisson, David Mendoza-Cozatl

Iron availability within the leaf vasculature determines the magnitude of iron deficiency responses in source and sink tissues in Arabidopsis.

Nga T. Nguyen[1,*], Mather A. Khan[1], Norma A. Castro-Guerrero[1], Ju-Chen Chia[2], Olena K. Vatamaniuk[2], Stephane Mari[3], Silvia S. Jurisson[4], David G. Mendoza-Cozatl[1,*]

[1]Division of Plant Sciences, University of Missouri-Columbia, 1201 Rollins St, Bond Life Sciences Center, Room 271F, Columbia, Missouri 65211, U.S.A.

[2]Soil and Crop Sciences Section, School of Integrative Plant Science, Cornell University, Ithaca, New York 14853, U.S.A.

[3]Biochimie et Physiologie Moleculaire des Plantes, INRAE, Montpellier, France.

[4]Department of Chemistry, University of Missouri-Columbia, Chemistry Building, Room 57, Columbia, MO 65211, U.S.A.

[*] Corresponding authors: N.T.N (ntnwbc@mail.missouri.edu) and D.G.M-C (mendozad@missouri.edu)

Short title: Local Fe deficiency responses in source and sink tissues

Corresponding authors:

D. G. Mendoza-Cozatl
Division of Plant Sciences,
University of Missouri-Columbia
1201 Rollins St, Bond-Life Sciences Center, Room 271F
Columbia, MO 65211, U.S.A.
Phone: (+1) 573-882 1892; Email: mendozad@missouri.edu

N. T. Nguyen
Division of Plant Sciences,
University of Missouri-Columbia
503 S. College Ave, Schweitzer Hall, Room 117
Columbia, MO 65211, U.S.A.
Email: ntnwbc@mail.missouri.edu

Abstract: Iron (Fe) uptake and translocation in plants are fine-tuned by complex mechanisms that are not yet fully understood. In *Arabidopsis thaliana*, local regulation of Fe homeostasis at the root level has been extensively studied and is better understood than the systemic shoot-to-root regulation. While the root system is solely a sink tissue that depends on photosynthates translocated from source tissues, the shoot system is a more complex tissue, where sink and source tissues occur synchronously. In this study, to gain better insight into the Fe deficiency responses in leaves, we overexpressed ZIP5, an Fe/Zn transporter, in phloem-loading cells (pro*SUC2*::At*ZIP5*) and determine the timing of Fe deficiency responses in sink (young leaves and roots) and source tissues (leaves). Transgenic lines overexpressing *ZIP5* in companion cells displayed increased sensitivity to Fe deficiency in root growth assays. Moreover, young leaves and roots (sink tissues) displayed either delayed or dampened transcriptional responses to Fe deficiency compared to wild type plants. We also took advantage of the Arabidopsis mutant *nas4x-1* to explore Fe transcriptional responses in the opposite scenario, where Fe is retained in the vasculature but in an unavailable and precipitated form. In contrast to pro*SUC2*::At*ZIP5* plants, *nas4x-1* young leaves and roots displayed a robust and constitutive Fe deficiency responses, while mature leaves showed a delayed and dampened Fe deficiency response compared to wildtype plants. Altogether, our data provide evidence suggesting that Fe sensing in leaves can also occur locally and in a leaf-specific manner.

Keywords: *Arabidopsis thaliana*, iron deficiency responses, leaf vasculature, phloem-loading cells, source and sink tissues, systemic signaling

Accession numbers: Information about *Arabidopsis thaliana* genes and proteins that are directly relevant to this study, including *ZIP5* (AT1G05300), *SUC2* (AT1G22710), *NAS1* (AT5G04950), *NAS2* (AT5G56080), *NAS3* (AT1G09240), *NAS4* (AT1G56430), *OPT3* (AT4G16370), *bHLH100* (AT2G41240), *FRO3* (AT1G23020), *FRO2* (AT1G01580), and *IRT1* (AT4G19690) can be retrieved from The Arabidopsis Information Resource (TAIR) at https://www.arabidopsis.org/.

Introduction

Iron (Fe) is an essential element for plants and organisms across all kingdoms. Plants are also the main source of Fe for other organisms, including humans. The majority of life on Earth depends on the capacity of plants to mine Fe from the Earth's crust and make it available for uptake and allocation within plant tissues. Iron is needed in multiple biological processes, including photosynthesis, respiration, DNA replication, and cell cycle control (Zhang, 2014, López-Millán et al., 2016); Despite the importance of Fe regulation in plants, our understanding of the molecular mechanisms that regulate Fe homeostasis in plants have just begun to be fully unraveled. Iron deficiency in humans (i.e. anemia) affects close to 2 billion people around the globe and a better understanding of the Fe homeostatic networks in plants will help developing crops with enhanced Fe content.

Iron uptake in dicot species such as Arabidopsis, relies on what is known as a *reducing strategy* or Strategy I where Fe, in the form of Fe^{3+}-insoluble complexes, is first reduced to Fe^{2+} by FRO2 (FERRIC REDUCTION OXIDASE 2) which is the substrate of IRT1 (IRON-REGULATED TRANSPORTER 1), the main Fe^{2+} transporter in Arabidopsis roots (Eide et al., 1996, Robinson et al., 1999, Henriques et al., 2002, Varotto et al., 2002, Vert et al., 2002). These two proteins, together with additional proteins such H(+)-ATPases (PLASMA MEMBRANE PROTON ATPASEs/ AHAs), coumarins and coumarin transporters, allow Arabidopsis to thrive in environments with different levels of Fe availability (Santi and Schmidt, 2009, Ziegler et al., 2017, Rosenkranz et al., 2021, Robe et al., 2021). From the different components that mediate Fe uptake in Arabidopsis, the regulation of IRT1 and FRO2, at transcriptional and post-transcriptional level, is perhaps one of the better studied ones. For instance, the transcription factor FIT has been described as a master regulator of the Fe deficiency responses in roots and is required to induce *IRT1* and *FRO2* during Fe deficiency (Colangelo and Guerinot, 2004). However, FIT alone is unable to induce the transcription of *IRT1* and *FRO2*. In turn, FIT needs to interact with members of the Ib subgroup of bHLH transcription factors (bHLH38/39/100/101) to promote transcriptional activation of the Fe uptake machinery (Yuan et al., 2008, Sivitz et al., 2012). This Ib subgroup of transcription factors is thought to be regulated upstream by members of the IVc subgroup of bHLH transcription factors (bHLH34/104/105/115), which together with the recently discovered Upstream Regulator of IRT1 (URI; bHLH121), completes the transcriptional network required to mount an Fe deficiency response in roots (Long et al., 2010, Zhang et al., 2015, Selote et al., 2015, Li et al., 2016, Kim et al., 2019, Gao et al., 2020). Notably, bHLH38/39/100/101 are also induced by Fe deficiency in

leaves, but FIT is preferentially expressed in roots suggesting that a yet unidentified FIT-like transcription factor may be needed in leaves to properly respond to Fe deficiency (Khan et al., 2018).

Other molecular players like BTS and BTS-like proteins also play an important role during Fe deficiency by regulating the turnover of IVc subgroup of bHLH transcription factors and preventing a constitutive activation of the Fe uptake machinery (Selote et al., 2015, Hindt et al., 2017; Rodriguez-Celma et al., 2019). FIT and URI are also known to be post-transcriptionally regulated by phosphorylation, and in case of FIT, CPK11 was identified as the kinase responsible for its phosphorylation (Gratz et al., 2019). Post-transcriptional regulation has also been demonstrated to regulate the activity and cellular localization of IRT1, and an impairment of these mechanisms results in either an inadequate response to Fe deficiency or a deregulated rate of Fe uptake that eventually leads to plant death (Barberon et al., 2011, Ivanov et al., 2014). All these layers of complexity should not be unexpected as the boundaries between Fe deficiency, sufficiency, and excess, are very narrow compared to other nutrients (Mendoza-Cózatl et al., 2019).

Regulation of Fe uptake at the root level, particularly the IRT1 post-transcriptional modifications is considered a *local response;* however, research in Arabidopsis and other plant species have shown that Fe homeostasis is also regulated *systemically* (Vert et al., 2002, Vert et al., 2003, Mendoza-Cózatl et al., 2014, Zhai et al., 2014, Gayomba et al., 2015). For instance, grafting experiments in sunflower and cucumber plants demonstrated that Fe deficiency in roots could be suppressed by grafting the shoot of an Fe sufficient plant onto a root experiencing Fe deprivation (Romera et al., 1992). Similarly, foliar application of Fe was able to suppress Fe deficiency in roots of Arabidopsis, tobacco, pea, tomato, and cucumber plants (Enomoto et al., 2007, García et al., 2013). These seminal experiments and others suggest that the *systemic* Fe signaling can override the local *root* signaling, at least at the transcriptional level. Notably, the molecular nature of this phloem-mobile signal has not been unequivocally identified. In contrast, there is a wealth of information about transporters and molecules required to keep Fe soluble for source-to-sink transport. For instance, nicotianamine (NA) is an Fe chelator synthesized by a family of nicotianamine synthases (NAS1/2/3/4), and the Arabidopsis quadruple mutant *nas4x-1* shows severe interveinal chlorosis during Fe deficiency, suggesting that NA is required for long-distance transport of Fe (Klatte et al., 2009, Schuler et al., 2012). In addition, Fe-NA complexes are transported by a family of transporters known as a Yellow Stripe-Like (YSL) proteins and the double mutant *ysl1 ysl3* showed impaired Fe homeostasis and lower Fe

in seeds (Jean et al., 2005, Waters et al., 2006, Chu et al., 2010, Kumar et al., 2017). More recently, the phloem-loading transporter OPT3 was identified as a key component of the Fe systemic signaling, and Arabidopsis mutants with residual levels of *OPT3* expression (*opt3-2* and *opt3-3*) display a constitutive upregulation of the Fe uptake machinery in roots (Mendoza-Cózatl et al., 2014, Zhai et al., 2014). However, no upstream regulators of *OPT3* or *YSLs* have been identified. Lastly, a family of peptides named IRON MAN were found to be mobile between shoots and roots and have been proposed to also play a role in the Fe systemic signaling (Hirayama et al., 2018, Grillet et al., 2018), by interacting with BTS and preventing the degradation of bHLH105/115 to preserve Fe homoeostasis (Li et al., 2021). In addition, URI/bHLH121 binds to the promoter region of IMA1/FEP3, suggesting that URI may also play a role in regulating the transcriptional activity of these phloem-mobile peptides in leaves (Kim et al., 2019).

In this study, we aimed to disrupt Fe homeostasis in the leaf vasculature to explore further and isolate the role of mature leaves in the regulation of Fe deficiency responses in source and sink tissues within then whole plant. We achieved this by overexpressing an Arabidopsis Fe transporter (*AtZIP5*) under the control of a phloem-specific promoter (*SUC2p*). AtZIP5 belongs to the Zinc/Iron-regulated transporter-like Protein (ZIP) gene family, ubiquitous among species and across kingdoms, including fungi, animals and plants [for a review see (Guerinot, 2000)]. The Arabidopsis genome harbors 15 ZIP members, twelve of them annotated as ZIP, from 1 to 12, and three IRT transporters (IRT1/2/3). While *AtZIP5* expression is downregulated during Fe deficiency, the use of the *SUC2p* allowed us to maintain a steady expression of *AtZIP5* in companion cells, even during Fe deprivation (Wintz et al., 2003, Dinneny et al., 2008, Long et al., 2010). Our results show that local disturbances of Fe levels in or around the vasculature of source leaves impacted the timing and magnitude of Fe deficiency responses and that these differences are unique between source (i.e. mature leaves) and sink tissues (i.e. young leaves and roots). We also performed similar experiments in the Arabidopsis mutant *nas4x-1*, which has residual levels of NA and therefore Fe precipitates in the vasculature of mature leaves, thus limiting Fe transport to sink tissues. In contrast to *SUC2p*::At*ZIP5* lines, *nas4x-1* mutants showed exacerbated Fe deficiency responses in sink tissues but dampened responses in mature leaves. Altogether, our data provide further evidence to suggest that Fe sensing in leaves can also occur *locally* in a leaf-specific manner, and that only mature leaves influence the *systemic* signaling driving Fe deficiency responses in roots.

Results

AtZIP5 is a plasma membrane transporter expressed in the vasculature.

Arabidopsis *ZIP5* (At*ZIP5*) is a member of the Zinc-regulated Iron-regulated transporter-like Protein family (ZIP), and members of this family have been shown to have the capacity to transport transition metals like iron (Fe) and Zinc (Zn). To test whether AtZIP5 was in fact capable of mobilizing Fe into cells, we expressed AtZIP5 in the *Saccharomyces cerevisiae* yeast strain *fet3 fet4,* a yeast mutant impaired in Fe uptake. Figure 1A shows that *fet3 fet4* yeast expressing AtZIP5 were able to grow on a medium with limited Fe availability (**Figure 1A**). Also, yeast cells expressing At*ZIP5* accumulated significantly higher levels of Fe compared to cells transformed with an empty vector and grown in medium supplemented with 100 µM of $FeCl_3$. Notably, the Fe concentration in ZIP5-expressing cells was comparable to the Fe levels found in wildtype yeast or *fet3 fet4* cells expressing At*IRT1* (**Figure 1B**). Because members of the ZIP family are known to transport other divalent metals, AtZIP5 was also tested for its capacity to transport Zn and Mn in yeast. When expressed in *zrt1 zrt2*, a yeast mutant defective in Zn transport, AtZIP5 was able to rescue yeast growth under limiting Zn availability; however, AtZIP5 was unable to complement the yeast mutant *smf1*, defective in Mn transport (**Figure S1**). These results show that AtZIP5 is a functional Fe/Zn transporter similar to AtIRT1.

Previous cell-specific translatome analyses found that *AtZIP5* was preferentially expressed in the vasculature ((Mustroph et al., 2009); **Figure S2A**). To experimentally verify this observation, we generated stable transgenic lines expressing the GUS reporter gene under the control of the *AtZIP5* promoter region (2.5 kb upstream of the transcription start site). Histochemical analysis of GUS activity in several independent T3 homozygous plants showed that *AtZIP5* expression is restricted to the vasculature (**Figure 2A-B**). Next, we aimed to confirm the cellular localization of AtZIP5 by expressing a translational fusion of the yellow fluorescent protein (*YFP*) and the coding sequence of At*ZIP5* (*YFP-AtZIP5*) in *Nicotiana benthamiana* (**Figure 2D-F**). The plasma membrane marker *PIP2A-mCherry* was also co-infiltrated with *YFP-AtZIP5* and used as a reference to localize plasma membrane proteins. Three days after co-infiltration, fluorescence was examined by confocal microscopy and a strong overlapping fluorescence signal was found between the plasma membrane marker PIP2A-mCherry and YFP-AtZIP5 (**Figure 2D-E**). The co-localization of PIP2A-mCherry and YFP-AtZIP5 was further corroborated by fluorescence

intensity plots showing two overlaping peaks corresponding to two adjacent adjacent cells (**Figure 2F**), suggesting that in plants, AtZIP5 is a plasma membrane transporter.

Phloem-specific expression of At*ZIP5* induces hypersensitivity to Fe deficiency.

Our previous studies have indicated that Fe availability at the whole plant level is primarily sensed in the leaf vasculature followed by a corresponding transcriptional response in roots (Khan et al., 2018). To further advance our understanding of shoot-to-root Fe deficiency responses, we wanted to test the timing and magnitude of the Fe deficiency responses in source and sink tissues of plants overexpressing an Fe transporter in the vasculature. However, AtZIP5 is induced by Fe excess (**Figure S2B-C**) and not deficiency (Wintz et al., 2003, Dinneny et al., 2008, Long et al., 2010) ; therefore, to by-pass this transcriptional regulation while keeping the tissue specificity, we generated independent transgenic lines expressing At*ZIP5* under the control of the phloem-specific promoter At*SUC2*. Previous whole-genome expression analyses shown that *SUC2* expression remains steady when plants over accumulate Fe and during Fe deficiency-like conditions such as Cd exposure (Khan et al., 2018; **Figure S3A**), thus the *SUC2p* offered the ideal means to maintain a constitutive vascular-specific expression of AtZIP5 during changes in Fe availability. Two independent T3 homozygous *SUC2p*::AtZIP5 lines, *ZIP5ox 16-10* and *ZIP5ox 25-5*, were selected for further characterization based on their strong ZIP5 expression detected by RT-PCR **(Figure S3B).**

To begin the characterization of the *SUC2p*::AtZIP5 lines (*ZIP5ox* lines), we first tested whether the overexpression of At*ZIP5* in the vasculature had an effect on the ability of plants to grow on Fe limiting conditions. Interestingly, both *ZIP5ox* lines displayed higher sensitivity to Fe deprivation compared to wildtype (WT, Col-0) (**Figure 3B)**. While roots of *ZIP5ox* lines were shorter than WT plants, no significant difference in Fe, Zn or Mn accumulation at the whole-plant level were detected between *ZIP5ox* lines and WT (**Figure S4)**, suggesting that the observed sensitivity to Fe deficiency is not associated with a major distribution of Fe within the plant but rather a more discrete, and perhaps localized disturbance of Fe availability in or around the vasculature.

Constitutive expression of At*ZIP5* in companion cells alters the Fe deficiency response in young leaves, mature leaves, and roots

Next, we analyzed Fe deficiency responses in WT and *ZIP5ox* lines. These experiments were conducted in 4-week-old plants grown hydroponically where young *sink* leaves can be separated from mature *source* leaves and roots to better dissect transcriptional responses at a tissue-specific manner (*see* **Figure S5** for a detailed description of leaf selection). Furthermore, to minimize the variation in the magnitude of Fe deficiency responses associated with circadian regulation, all Fe deficiency experiments were started in the morning (T0), more specifically two hours after the light in the growth chamber was turned on (i.e. ZT2). Three well-documented vascular markers for Fe deficiency in leaves (*OPT3*, *bHLH100,* and *FRO3*) (**Figure S6** and Khan et al. 2018) were used to quantify the timing and magnitude of the Fe deficiency responses in *ZIP5ox* lines and WT plants. In some cases, *ZIP5ox* lines showed a constitutively lower level of expression of these Fe deficiency marker genes, even in Fe replete conditions (**Figure 4**). For instance, *ZIP5ox* young leaves had a lower expression level of *bHLH100* at T0 (i.e., the beginning of the experiment). Similarly, *OPT3* and *bHLH100* expression were also lower in mature leaves of *ZIP5ox* lines compared to WT (**Figure 4A-B**). These differences were small yet significant and consistent in both *ZIP5ox* lines.

During Fe deficiency, two major trends were identified in leaves. First, independent of the genotype, *OPT3*, *bHLH100*, and *FRO3* expression were induced throughout the Fe deficiency experiments (**Figure 4A-C**), indicating that our Fe deficiency treatment was effective and properly sensed by all genotypes. Second, and related to the magnitude of Fe deficiency responses, we found that young leaves of *ZIP5ox* plants displayed a reduced response (measured as lower expression levels of *OPT3*, *bHLH100*, and *FRO3*) during Fe deficiency compared to WT young leaves at both 12 hr and 24 hr of Fe deprivation (**Figure 4A-C**). *ZIP5ox* mature leaves, on the other hand, had a similar Fe deficiency response than WT at the 12 hr time point, but this response was clearly dampened at the 24 hr time-point. Overall, the expression data from leaves indicate that overexpressing At*ZIP5* in the vasculature decreased the magnitude of the Fe deficiency response in leaves.

In roots, the Fe deficiency response was assessed by following the expression of two well-known Fe deficiency markers: *FRO2* and *IRT1*. Similar to leaves, all plant genotypes displayed an increased expression of *FRO2* and *IRT1* during Fe deprivation, and *ZIP5ox* lines had lower levels of expression of *FRO2* and *IRT1* compared to WT. Moreover, the magnitude of the Fe deficiency response in *ZIP5ox* roots after 12 hrs of Fe

deficiency was significantly lower than WT. After 24 hr, both *IRT1* and *FRO2* reached levels of expression similar to WT suggesting that overexpression of At*ZIP5* in the vasculature delayed, but did not inhibit, the full magnitude of Fe deficiency responses in roots.

Nicotianamine deficiency uncouples Fe deficiency responses in young leaves and mature leaves.

To further test the *autonomous* magnitude of Fe deficiency responses in source and sink tissues, we took advantage of the Arabidopsis *nas4x-1* mutant, which has only trace levels of nicotianamine (Klatte et al., 2009, Schuler et al., 2012). Nicotianamine (NA) is an Fe chelator required for source-to-sink mobilization of Fe and in this case, the *nas4x-1* mutant represents an opposite scenario compared to *ZIP5ox* lines, as the lack of NA results in precipitation of the Fe within the vasculature, thus reducing the levels of Fe available for long-distance transport. To further characterize *ZIP5ox* lines and *nas4x-1* mutant and to explore the distribution of Fe between young and mature leaves, both genotypes were subjected to X-ray fluorescence spectrometry (XRF). While no major changes were observed in young leaves of *nas4x-1* or *ZIP5ox* lines (**Figure S7**), higher levels of Fe were detected within the vasculature of *nas4x-1* mature leaves (**Figure 5A**). In contrast, *ZIP5ox* lines showed a consistent lower signal of Fe (shown as pixel intensity) particularly in the vasculature near the edge of the leaf (Figure 5B-C). A similar trend was found for Zn but not for Ca, Cu, K and Mn (**Figure S8**). The overaccumulation of Fe *nas4x-1* in mature leaves was consistent with Fe levels measured by ICP-OES (**Figure S9**), where young leaves of the *nas4x-1* mutant showed lower levels of Fe while mature leaves showed a higher accumulation of Fe. Moreover, shoot-to-root ^{59}Fe mobilization experiments indicated that *nas4x-1* plants have a lower ability to translocate Fe between mature leaves and roots (**Figure 5D**).

Next, we used the same Fe deficiency markers previously described to assess the Fe deficiency response in young leaves, mature leaves, and roots of *nas4x-1* (**Figure 6**). Interestingly, our results showed striking differences between young and mature leaves. For instance, *nas4x-1* young leaves displayed a constitutive Fe deficiency response, where *OPT3*, *bHLH100*, and *FRO3* were up-regulated at all tested time-points (**Figure 6A-C**). In *nas4x-1* mature leaves however, the expression of all the Fe deficiency markers was consistently lower compared to WT. For instance, at T0, the expression of *OPT3* was similar between *nas4x-1* and WT; however, the magnitude of Fe-deficiency responses in *nas4x-1* mature leaves was significantly lower than in WT mature leaves. A similar trend

was found for *bHLH100* and *FRO3* expression (**Figure 6B-C**); that is, *nas4x-1* mature leaves displayed a slightly but significantly higher expression of *bHLH100* and *FRO3* compared to Col-0 mature leaves at T0. Moreover, under Fe deficiency, *nas4x-1* mature leaves had a smaller magnitude of Fe deficiency response at the 12 hr time-point compared to wildtype. At the 24 hr time-point, this difference was reduced between genotypes and the expression levels of both *bHLH100* and *FRO3* were similar between mature leaves of *nas4x-1* and WT.

In addition, and similar to the expression of *OPT3* in young leaves, *bHLH100* and *FRO3* were also constitutively up-regulated in *nas4x-1* young leaves and, during Fe deficiency, the magnitude of the transcriptional response was higher compared to WT leaves (**Figure 6A-C**). A similar response was found in roots, where the expression of *FRO2* and *IRT1* was higher in *nas4x-1* than WT at all tested time-points, and the magnitude of the Fe deficiency response was also higher compared to WT (**Figure 6D**). Overall, the *nas4x-1* results are consistent with a model where sink tissues (i.e., young leaves and roots) are constitutively deprived of Fe due to the lack of NA. Perhaps more interestingly, we found two additional facts: (1) the typical Fe deficiency response observed in WT plants is far from saturation as the magnitude of the Fe deficiency response in *nas4x-1* was higher than WT. These results suggest that Fe deficiency responses are continuously and negatively regulated in WT plants even during Fe deprivation. These negative regulators are yet to be identified. (2) Moreover, *nas4x-1* plants have less mobile Fe in the phloem, yet vascular-localized Fe deficiency markers such as *OPT3*, *bHLH100,* and *FRO3* are constitutively repressed in mature leaves, where Fe is deposited around the vasculature. These results suggest that high levels of Fe *outside* companion cells can override what should have been an Fe deficiency response, triggered by low levels of Fe *inside* companion cells. It is therefore possible that a portion of the Fe sensing mechanism in mature leaves occurs on the apoplastic side of the vasculature.

Discussion

For decades, systemic shoot-to-root signaling has been known to regulate Fe uptake at the root level in Arabidopsis and other dicot species (Romera et al., 1992, Vert et al., 2003, Enomoto et al., 2007, García et al., 2013). However, very few details about the molecular mechanisms behind this systemic regulation are known to date. In contrast, several molecular players of the Fe uptake machinery together with their associated transcriptional and post-transcriptional regulators in roots have been described. For instance, recent data have revealed at least two

layers of transcriptional regulation controlling the expression of *IRT1* and *FRO2* during Fe starvation. These two layers include members of the Ib subgroup of bHLH transcription factors (bHLH38/39/100/101), which in coordination with members of the IVc subgroup of bHLH transcription factors (bHLH34/104/105/115), regulate the Fe uptake machinery in roots (Yuan et al., 2008, Sivitz et al., 2012, Long et al., 2010, Zhang et al., 2015, Selote et al., 2015, Li et al., 2016). In addition, *local* and post-transcriptional regulation of some of these transcription factors, such as URI and FIT, and ubiquitination of IRT1 also contribute to the fine-tuning regulation of Fe homeostasis in roots (Barberon et al., 2011, Kim et al., 2019, Gao et al., 2020).

The *systemic* shoot-to-root regulation of Fe homeostasis, on the other hand, is far less understood compared to roots, but evidence from Arabidopsis and other dicot plants suggest that the systemic signaling dictates, and may even override, the local response to Fe deficiency in roots (Romera et al., 1992, Enomoto et al., 2007, García et al., 2013). The entire root system is by definition a *sink* tissue, as it depends on the energy (i.e. photosynthates) assimilated and translocated from *source* leaves. In contrast, the shoot system is a more diverse and complex tissue, where sink and source tissues occur synchronously. For instance, young developing leaves are *sink* tissues that depend on *source* leaves for an adequate supply of energy and nutrients to sustain growth and development. In a sense, young developing leaves are in continuous demand for Fe and could be considered constitutively Fe deficient during their transition from sink to source leaves. This co-occurrence of source and sink tissues within the shoot system may explain in part why only a few players of the Fe deficiency response in leaves have been identified. After all, it is not uncommon to use the entire shoot system in whole-genome transcriptome analyses, but the shoot system may be displaying different timing and magnitude of transcriptional changes, and even opposite changes, in a leaf-specific manner, thus canceling relevant changes if the entire shoot system is used in whole-genome expression analysis.

Here we aimed to disturb local levels of Fe availability by expressing an Fe transporter (AtZIP5) specifically in companion cells. We were particularly interested in dissecting the responses in a tissue-specific manner, including source leaves (mature leaves) and sink tissues such as young leaves and roots. Our results demonstrate that AtZIP5 is an Fe/Zn transporter preferentially expressed in the vasculature (**Figures 1 and 2**). At*ZIP5,* however, is natively up-regulated during Fe excess, not Fe deficiency (**Figure S2B-C**); therefore, to better control the transcription of At*ZIP5*, we generated transgenic Arabidopsis plants expressing At*ZIP5* under the control

of the phloem-specific *SUC2* promoter, which is expressed only in source leaves and whose transcription is independent of the Fe status of the plant (Figures S3A). Interestingly, *ZIP5ox* plants displayed hypersensitivity to Fe deficiency in root growth assays (**Figure 3**). During Fe deficiency, leaves transmit an unknown signal to roots to either up-regulate or repress Fe uptake at the root level. It is possible that expression of AtZIP5 in phloem-loading cells prevented the up-regulation of Fe deficiency responses by altering Fe levels in or around the vasculature in source leaves. This suggestion is supported by the transcriptional responses of Fe deficiency markers in sink tissues, where young leaves and roots show either delayed or dampened responses to Fe deficiency compared to WT plants (**Figure 4**). In addition, and similar to other ZIP transporters, ZIP5 is able to mobilize both Fe and Zn and although Zn levels were not affected at the whole tissue level (Figure S4B), it is possible that the observed Fe deficiency responses in ZIP5ox plants are also the result of more complex yet unknown interactions between transition elements and their sensing mechanisms (Lešková et al. 2022).

To explore the opposite scenario, we took advantage of the Arabidopsis *nas4x-1* mutant, which is known to have low mobility of Fe between source and sink tissues due to the residual levels of NA at the whole plant level (Klatte et al., 2009, Schuler et al., 2012). Thus, *nax4x-1* provides an opposite scenario compared to *ZIP5ox* lines, where Fe is preferentially retained at high levels in mature leaves with only residual transport to young leaves. This scenario was confirmed by elemental imaging using XRF, which demonstrates that Fe is retained in the vasculature of *nax4x-1* mature leaves (**Figure 5B**). In turn, sink tissues such as young leaves and roots display a faster and stronger Fe deficiency response compared to the delayed and dampened response of mature leaves. Notably, this study, together with previous studies, emphasize the need to address Fe deficiency responses in a leaf-specific manner (Klatte et al., 2009, Chu et al., 2010, Schuler et al., 2012, Kumar et al., 2017). Moreover, there is now sufficient evidence, including this work, to suggest that each leaf within the shoot system may respond in unique ways (i.e., *local* Fe sensing in leaves) depending on their access to Fe availability and other environmental cues (Schuler et al., 2011, Hantzis et al., 2018). This may be explained by the fact that young leaves are under development and therefore have a higher demand for Fe; thus, young leaves are more prone to trigger Fe deficiency responses by small changes in Fe levels compared to the changes needed to trigger an equivalent response in mature leaves. Moreover, one of the early responses to Fe deficiency in mature leaves is a reduced mobilization of Fe to young leaves, which may enhance the Fe starvation experienced by sink leaves.

Similar to *nax4x-1,* the double mutant *ysl1 ysl3* also accumulates significant levels of Fe within the vasculature (Kumar et al., 2017). YSL1 and YSL3, are metal-nicotianamine transporters preferentially expressed in the vasculature and are thought to be important for source-to-sink transport of Fe as the *ysl1 ysl3* mutant shows reduced levels of Fe, Zn and Cu in seeds (Waters et al., 2006). However, and in contrast to *nas4x-1*, the *ysl1 ysl3* double mutant is unable to induce an Fe deficiency response when Fe availability is reduced. It has been suggested that YSL1/3 may have a role in unloading metal-NA complexes from the vasculature and therefore the increased levels of Fe in the phloem in *ysl1 ysl3* may be repressing, constitutively, the Fe deficiency response in roots. The difference between *nas4x-1* and *ysl1 ysl3* mutants in terms of transcriptional responses during Fe deficiency can also be explained in terms of solubility as *ysl1 ysl3* are not impaired in NA synthesis and therefore, NA in the phloem should maintain a proportion of Fe in an available soluble form. In contrast, *nas4x-1* has functional YSL1 and YSL3 transporters but the low levels of NA in the vasculature likely favors Fe precipitation, thus reducing the effective concentration of mobile Fe in the phloem. An additional layer of complexity comes from the fact that high levels of Fe lead to the production of reactive oxygen species and these have been found to repress Fe deficiency responses in leaves and roots (Le at la., 2016; McInturf et al., 2021). Altogether, these observations illustrate the complexity and hierarchical structure of Fe deficiency responses in plants, which is expected considering the high reactivity of Fe. It is also a reminder that as of today, there is no data about Fe speciation in the phloem sap other than predictions and the identification and quantification of the different soluble forms of Fe is critical to understand the systemic nature of shoot-to-root Fe signaling in plants.

Historically, the identification of molecular mechanisms behind Fe deficiency responses in roots has been more advanced compared to our understanding of Fe deficiency responses in leaves. In hindsight, this should have been expected as the root system is a more homogeneous tissue compared to shoots. In fact, initial experiments that took advantage of the first whole-genome transcriptome technologies, like the Affymetrix microarray chips, were sufficient to identify key transcription factors regulating Fe deficiency responses in roots (Colangelo and Guerinot, 2004, Long et al., 2010). Not surprisingly, similar approaches have not provided the same level of information for leaves. However, it is now clear that Fe deficiency responses in shoots can also be *autonomous* and leaf specific. Moreover, and due to the directional movement of nutrients between sink and source tissues, it is likely that source leaves, but not young leaves, play a major role in Fe homeostasis by sensing the Fe levels at the whole plant level to systemically regulate Fe uptake in roots (Mendoza-Cózatl et al., 2014, Zhai et al., 2014, Khan et al., 2018). These

observations, together with current *-omic* approaches at a tissue- and cell-specific resolution, offer a renewed opportunity to study Fe homeostasis from a *systems level* perspective, and may get us all closer – as a field – to a better understanding of the molecular mechanisms behind Fe sensing and Fe homeostasis in plants, at the whole plant level.

Materials and Methods

Plant growth conditions

Surface-sterilized seeds from Arabidopsis Col-0 were geminated on one-quarter Murashige and Skoog (MS) medium after stratification for 2-days in 4^{o}C/ dark condition. The light setting used throughout the study was 16 h light/ 8 h dark condition with 23°C day/ 21°C night, and the growth chamber humidity was maintained at 60 %. When seedlings have two true leaves (10-12 days after seed plating), plants were transferred to a hydroponic setup with 50 µM Fe-EDTA as described in Nguyen et al. (2016). For the phenotypic test on Fe deficiency plates, minimal medium plates were prepared to have the same composition as the hydroponic solution but with 0.7 % phytoagar. Fe-deficiency plates contained 0.15 mM of ferrozine (Fe chelator) and were not supplemented with Fe. For elemental analysis, roots and leaves were collected from hydroponically grown plants (18-day post transferring seedlings to hydroponic setup) while seeds, seed husk were collected from soil-grown plants. The soil used in this study was growing medium PRO-MIX FLX manufactured by Premier Horticulture LTD. Arabidopsis *nas4x-1* mutants were kindly provided by Dr. Petra Bauer (Institute of Botany, Heinrich-Heine University).

Functional complementation assay in yeast

Saccharomyces cerevisiae fet3 fet4, zrt1 zrt2 and smf1 (kindly provided by Dr. David Eide, University of Wisconsin–Madison) were transformed with *pYES2 or pAG426GPD (*Addgene # 14156) plasmids carrying the coding sequence of either At*ZIP5* or At*IRT1* via the lithium acetate method (Schiestl and Gietz, 1989). Transformants were grown in selective media and the presence of the plasmid was verified by standard yeast-colony PCR. Yeast growth complementation assays were performed on selective media (Sunrise Science Products, TN, USA) lacking Fe (Cat# 1551-250), Zn (Cat# 1555-250) or Mn (Cat# 1539-250). In experiments were pYES2

plasmids were used, glucose was replaced by 2% galactose and 1% raffinose to activate the *GAL1* promoter, which drives the expression of the transgenes. To determine the Fe concentration in yeast cells, yeast were grown overnight in liquid cultures (-Fe, no iron added, or + Fe, supplemented with 100 μM of $FeCl_3$). Yeast cells were harvested and washed for one time with wash buffer (Tris 20 mM, EDTA 5mM, pH 8) and three times with DI water and brought to constant weight in an oven at 60 ˚C. Dehydrated cells were used for elemental analysis (ICP-OES) to quantify the micronutrient concentrations (Fe, Mn, Zn, Cu) and normalized by dry weight. Wildtype yeast and *fet3 fet4* yeast transformed with *IRT1* were used as positive controls.

Generation of Arabidopsis stable transgenic lines

To generate the *SUC2p::*At*ZIP5* construct, the At*ZIP5* coding sequence was amplified from cDNA of Col-0 plants using PCR and introduced into *pENTR/D-TOPO* plasmid (Gateway® entry clone) using the manufacturer recommendations. After the sequence was confirmed by Sanger sequencing, the At*ZIP5* coding sequence was mobilized to a modified *pGreen II 0179* plasmid where 2kb of the *SUC2p* promoter sequence had been inserted using the restriction enzymes KpnI/BamHI the Gateway cassette containing attLR sites (see Supplementary Table 1 for a detailed list of primers used).

To generate the *ZIP5p::GUS* construct, 2.5 kb genomic region upstream of *ZIP5* transcription start site was amplified from gDNA from the Col-0 ecotype by PCR and introduced into *pENTR/D-TOPO*. *ZIP5* promoter was later recombined into *pBGGUS* plasmid (Kubo et al., 2005) by an LR II clonase reaction.

Arabidopsis ecotype Col-0 plants were transformed independently with these constructs using the floral dip method as described in Clough and Bent (1998) using *Agrobacterium tumefaciens* strain GV3101, which carries the *pSoup* helper plasmid for *pGreen II*-carrying strains as described in Hellens et al. (2000). T3 homozygous lines were selected on hygromycin and T3 homozygous were identified by segregation analysis and transferred to soil for seed propagation.

Transient expression in *Nicotiana benthamiana* and fluorescence confocal imaging

*35Sp::YFP-*At*ZIP5* fusion was obtained by recombining the At*ZIP5* coding sequence into *pEarleyGate 104* (ABRC stock# CD3-686, *35Sp::YFP-Gateway-OCS* 3') using an LR reaction. The plasma membrane marker used in

this study was a full-length fusion of the aquaporin PIP2A to mCherry that was obtained from the ABRC stock center (Nelson et al., 2007). These constructs were transformed into *A. tumefaciens* strain GV3101 and used transient expression assaya. Leaves of *N. benthamiana* were co-infiltrated with YFP-AtZIP5 and PIP2A-mCherry as previously described in Wydro et al. (2006). 3-day post infiltration, the infiltrated area of the leaf was observed using a Leica TCP SP8 confocal microscope (60X magnification).

Histochemical GUS staining

For GUS staining, leaves and roots of transgenic plants carrying pro*ZIP5::GUS* were grown on hydroponics for two weeks under Fe sufficient condition. GUS staining was performed overnight with 2 mM X-Gluc (5-bromo-4-chloro-3-indolyl-β-d-glucuronide) as described in Mendoza-Cózatl et al. (2014). Staining patterns were analyzed using Leica M205 stereomicroscope.

Elemental analysis

Inductively coupled plasma - optical emission spectrometry (ICP-OES) was used to determine the elemental composition in yeast cells and plant samples. The protocol was described in Chen et al. (2006). Briefly, after collection, tissue samples were washed with buffer (Tris 20mM, EDTA 5mM, pH 8) and DI water to eliminate ions bound to the surface. Samples were then dried, weighed, and digested using HNO_3 70 %. Dilution of the digested samples in a homogeneous liquid phase (no debris) was brought to 10 mL and analyzed for Fe, Zn, Mn, and Cu concentrations by ICP-OES.

Gene expression analysis

Eighteen days after transferring to hydroponics, plants were moved to Fe deficient conditions. The Fe-sufficient hydroponic solution used in this study contains 50 µM of Fe-EDTA; Fe-deficient hydroponic solution had the same composition but without Fe. Roots of plants for Fe-deficiency treatment were gently washed with Fe-deficient hydroponic solution for 15 minutes on a shaker before starting the actual treatment. The hydroponic

solution used on the treatment day was prepared with Milli-Q water. Young leaves, mature leaves, and roots were collected separately as described in Figure S5. Plant tissues were collected for RNA extraction (Direct-zol™ RNA MiniPrep Plus kit, Zymo Research) and cDNA synthesis (SuperScript III® kit – Invitrogen). Gene expression analysis was performed by semi-quantitative PCR (RT-PCR) or quantitative real-time PCR (qRT-PCR) and normalized using At*ACT2* (AT3G18780) expression as described in Khan et al. (2018). Each biological replicate came from homogenized tissues of five to six plants. Results represent the mean of three biological replicates. Gene expression analysis data represent for three independent experiments.

^{59}Fe leaf-to-root transport assay

Hydroponically grown Col-0 and *nas4x-1* plants were used in a leaf-to-root transport assay. A big mature leaf (loaded leaf) from each plant was incubated with 0.5 mL buffer solution containing 50 mM MES, 15 µM $FeCl_3$ (non-radioactive form), 1 mM ascorbic acid, 2 mM sucrose, and 20 µCi $^{59}FeCl_3$ (pH~6). 2 hours after incubation, loaded leaves were carefully removed and washed one time with wash buffer (Tris 20mM, EDTA 5mM) and two times with DI water. Whole roots were removed from plants and gently placed on a tissue paper to remove the hydroponic solution. Fresh weight of the root samples was measured and recorded for normalization. ^{59}Fe activity in loaded leaves was measured using a dose calibrator. ^{59}Fe activity in root samples were measured using a liquid scintillation counter as described in Khan et al. (2018).

Synchrotron X-ray fluorescence (XRF) map of Fe distribution in leaves

The first (mature) and the sixth (young) leaves were harvested from 23-24 day-old plants grown hydroponically and leaves were placed in the wet chamber made between two layers of metal-free Kapton film. The spatial distribution of iron in hydrated leaf tissues was imaged via XRF at the F3 station at the Cornell High Energy Synchrotron Source (CHESS) as described in Kumar et al., 2017.

Data Availability

Information about *Arabidopsis thaliana* genes and proteins that are directly relevant to this study, including *ZIP5* (AT1G05300), *SUC2* (AT1G22710), *NAS1* (AT5G04950), *NAS2* (AT5G56080), *NAS3* (AT1G09240), *NAS4* (AT1G56430), *OPT3* (AT4G16370), *bHLH100* (AT2G41240), *FRO3* (AT1G23020), *FRO2* (AT1G01580), and *IRT1* (AT4G19690) can be retrieved from The Arabidopsis Information Resource (TAIR) at https://www.arabidopsis.org/. Visualization of whole-genome expression profiling datasets of *Arabidopsis* wildtype and *opt3-2* are available at http://artemis.cyverse.org/david_lab_efp/cgi-bin/efpWeb.cgi

Funding information

This research was supported in part by the US National Science Foundation (MCB-1818312 and IOS- 1734145 to D. M. C.). Radiotracer experiments using ^{59}Fe were supported through an NSF EPSCoR Track II award (IIA-1430428 to D. G. M-C. and S. S. J.) and by a grant from the Department of Energy (Projects for Interrogations of Biological Systems, DE-SC0002040 to S. S. J.). N. T. N. was supported by the Vietnam Education Foundation Training Program (Exchange visitor program No. G-3-10180). Parts of this research used the F3 Beamline at the Cornell High Energy Synchrotron Source (CHESS) which during the period of research was supported by the National Science Foundation under award DMR-1332208. Parts of this work in the O.K.V. lab was funded by NSF-IOS #1754966 and NSF-IOS #1656321.

ORCID

David G. Mendoza-Cozatl http://orcid.org/0000-0002-9616-0791

Nga T. Nguyen https://orcid.org/0000-0003-1016-3068

Olena K. Vatamaniuk: https://0000-0003-2713-3797

References

BARBERON, M., ZELAZNY, E., ROBERT, S., CONÉJÉRO, G., CURIE, C., FRIML, J. & VERT, G. 2011. Monoubiquitin-dependent endocytosis of the IRON-REGULATED TRANSPORTER 1 (IRT1) transporter controls iron uptake in plants. *Proceedings of the National Academy of Sciences,* 108**,** E450-E458.

CHEN, A., KOMIVES, E. & SCHROEDER, J. 2006. An improved grafting technique for mature Arabidopsis plants demonstrates long-distance shoot-to-root transport of phytochelatins in Arabidopsis. *Plant Physiology,* 141**,** 108-20.

CHU, H.-H., CHIECKO, J., PUNSHON, T., LANZIROTTI, A., LAHNER, B., SALT, D. E. & WALKER, E. L. 2010. Successful reproduction requires the function of Arabidopsis Yellow Stripe-Like1 and Yellow Stripe-Like3 metal-nicotianamine transporters in both vegetative and reproductive structures. *Plant physiology,* 154**,** 197-210.

CLOUGH, S. J. & BENT, A. F. 1998. Floral dip: a simplified method for Agrobacterium -mediated transformation of Arabidopsis thaliana. *The Plant Journal,* 16**,** 735-743.

COLANGELO, E. P. & GUERINOT, M. L. 2004. The essential basic helix-loop-helix protein FIT1 is required for the iron deficiency response. *Plant Cell,* 16.

DINNENY, J. R., LONG, T. A., WANG, J. Y., JUNG, J. W., MACE, D., POINTER, S., BARRON, C., BRADY, S. M., SCHIEFELBEIN, J. & BENFEY, P. N. 2008. Cell identity mediates the response of Arabidopsis roots to abiotic stress. *Science,* 320.

EIDE, D., BRODERIUS, M., FETT, J. & GUERINOT, M. L. 1996. A novel iron-regulated metal transporter from plants identified by functional expression in yeast. *Proc Natl Acad Sci USA,* 93.

ENOMOTO, Y., HODOSHIMA, H., SHIMADA, H., SHOJI, K., YOSHIHARA, T. & GOTO, F. 2007. Long-distance signals positively regulate the expression of iron uptake genes in tobacco roots. *Planta,* 227**,** 81-89.

GAO, F., ROBE, K., BETTEMBOURG, M., NAVARRO, N., ROFIDAL, V., SANTONI, V., GAYMARD, F., VIGNOLS, F., ROSCHZTTARDTZ, H., IZQUIERDO, E. & DUBOS, C. 2020. The Transcription Factor bHLH121 Interacts with bHLH105 (ILR3) and Its Closest Homologs to Regulate Iron Homeostasis in Arabidopsis. *The Plant Cell,* 32**,** 508-524.

GARCÍA, M. J., ROMERA, F. J., STACEY, M. G., STACEY, G., VILLAR, E., ALCÁNTARA, E. & PÉREZ-VICENTE, R. 2013. Shoot to root communication is necessary to control the expression of iron-acquisition genes in Strategy I plants. *Planta,* 237**,** 65-75.

GAYOMBA, S. R., ZHAI, Z., JUNG, H.-I. & VATAMANIUK, O. K. 2015. Local and Systemic Signaling of Iron Status and Its Interactions with Homeostasis of Other Essential Elements. *Frontiers in Plant Science,* 6.

GRATZ, R., MANISHANKAR, P., IVANOV, R., KÖSTER, P., MOHR, I., TROFIMOV, K., STEINHORST, L., MEISER, J., MAI, H. J., DRERUP, M., ARENDT, S., HOLTKAMP, M., KARST, U., KUDLA, J., BAUER, P. & BRUMBAROVA, T. 2019. CIPK11-Dependent Phosphorylation Modulates FIT Activity to Promote Arabidopsis Iron Acquisition in Response to Calcium Signaling. *Dev Cell,* 48**,** 726-740.e10.

GRILLET, L., LAN, P., LI, W., MOKKAPATI, G. & SCHMIDT, W. 2018. IRON MAN is a ubiquitous family of peptides that control iron transport in plants. *Nature Plants,* 4**,** 953-963.

GUERINOT, M. L. 2000. The ZIP family of metal transporters. *Biochimica et Biophysica Acta (BBA) - Biomembranes,* 1465**,** 190-198.

HANTZIS, L. J., KROH, G. E., JAHN, C. E., CANTRELL, M., PEERS, G., PILON, M. & RAVET, K. 2018. A Program for Iron Economy during Deficiency Targets Specific Fe Proteins. *Plant Physiology,* 176**,** 596-610.

HELLENS, R. P., EDWARDS, E. A., LEYLAND, N. R., BEAN, S. & MULLINEAUX, P. M. 2000. pGreen: a versatile and flexible binary Ti vector for Agrobacterium-mediated plant transformation. *Plant Molecular Biology,* 42**,** 819-832.

HENRIQUES, R., JÁSIK, J., KLEIN, M., MARTINOIA, E., FELLER, U., SCHELL, J., PAIS, M. S. & KONCZ, C. 2002. Knock-out of Arabidopsis metal transporter gene IRT1 results in iron deficiency accompanied by cell differentiation defects. *Plant Mol Biol,* 50.

HINDT, M. N., AKMAKJIAN, G. Z., PIVARSKI, K. L., PUNSHON, T., BAXTER, I., SALT, D. E. & GUERINOT, M. L. 2017. BRUTUS and its paralogs, BTS LIKE1 and BTS LIKE2, encode important negative regulators of the iron deficiency response in Arabidopsis thaliana. *Metallomics,* 9**,** 876-890.

HIRAYAMA, T., LEI, G. J., YAMAJI, N., NAKAGAWA, N. & MA, J. F. 2018. The Putative Peptide Gene FEP1 Regulates Iron Deficiency Response in Arabidopsis. *Plant and Cell Physiology,* 59**,** 1739-1752.

IVANOV, R., BRUMBAROVA, T., BLUM, A., JANTKE, A.-M., FINK-STRAUBE, C. & BAUER, P. 2014. SORTING NEXIN1 Is Required for Modulating the Trafficking and Stability of the Arabidopsis IRON-REGULATED TRANSPORTER1. *The Plant Cell,* 26**,** 1294-1307.

JEAN, M. L., SCHIKORA, A., MARI, S., BRIAT, J.-F. & CURIE, C. 2005. A loss-of-function mutation in AtYSL1 reveals its role in iron and nicotianamine seed loading. *The Plant Journal,* 44**,** 769-782.

KHAN, M. A., CASTRO-GUERRERO, N. A., MCINTURF, S. A., NGUYEN, N. T., DAME, A. N., WANG, J., BINDBEUTEL, R. K., JOSHI, T., JURISSON, S. S., NUSINOW, D. A. & MENDOZA-COZATL, D. G. 2018. Changes in iron availability in Arabidopsis are rapidly sensed in the leaf vasculature and impaired sensing leads to opposite transcriptional programs in leaves and roots. *Plant, Cell & Environment,* 41**,** 2263-2276.

KIM, J.-Y., SYMEONIDI, E., PANG, T. Y., DENYER, T., WEIDAUER, D., BEZRUTCZYK, M., MIRAS, M., ZÖLLNER, N., HARTWIG, T., WUDICK, M. M., LERCHER, M., CHEN, L.-Q., TIMMERMANS, M. C. P. & FROMMER, W. B. 2021. Distinct identities of leaf phloem cells revealed by single cell transcriptomics. *The Plant Cell,* 33**,** 511-530.

KIM, S. A., LACROIX, I. S., GERBER, S. A. & GUERINOT, M. L. 2019. The iron deficiency response in Arabidopsis thaliana requires the phosphorylated transcription factor URI. *Proceedings of the National Academy of Sciences,* 116**,** 24933-24942.

KLATTE, M., SCHULER, M., WIRTZ, M., FINK-STRAUBE, C., HELL, R. & BAUER, P. 2009. The analysis of Arabidopsis nicotianamine synthase mutants reveals functions for nicotianamine in seed iron loading and iron deficiency responses. *Plant physiology,* 150**,** 257-271.

KUBO, M,, UDAGAWA, M., NISHIKUBO, N., HORIGUCHI, G., YAMAGUCHI, M., ITO, J., MIMURA, T., FUKUDA, H., DEMURA, T. 2005 Transcription switches for protoxylem and metaxylem vessel formation. Genes and Development 19:1855-60.

KUMAR, R. K., CHU, H.-H., ABUNDIS, C., VASQUES, K., RODRIGUEZ, D. C., CHIA, J.-C., HUANG, R., VATAMANIUK, O. K. & WALKER, E. L. 2017. Iron-Nicotianamine Transporters Are Required for Proper Long Distance Iron Signaling. *Plant Physiology,* 175**,** 1254-1268.

LE C.T., BRUMBAROVA, T., IVANOV, R., STOOF, C., WEBER, E., MOHRBACHER, J., FINK-STRAUBE, C., BAUER, P. (2016) Zinc finger of Arabidopsis thaliana12 (zat12) interacts with Fer-like Iron deficiency-induced Transcription factor (FIT) linking iron deficiency and oxidative stress responses. *Plant Physiology* 170:540-57.

LEŠKOVÁ, A., JAVOT, H., GIEHL, R.F.H. (2022) Metal crossroads in plants: modulation of nutrient acquisition and root development by essential trace metals. Journal of Experimental Botany. 73:1751-1765.

LI, X., ZHANG, H., AI, Q., LIANG, G. & YU, D. 2016. Two bHLH Transcription Factors, bHLH34 and bHLH104, Regulate Iron Homeostasis in Arabidopsis thaliana. *Plant Physiology,* 170**,** 2478-2493.

LI, Y., LI, Y., LU, C.K., LI, C.Y., LEI, R.H., PU, N., ZHAO, J.H., PENG, F., PING, H.Q., WANG, D., LIANG, G. 2021 IRON MAN interacts with BRUTUS to maintain iron homeostasis in Arabidopsis. *Proceedings of the National Academy of Sciences* 2021 Sep 28;118(39):e2109063118.

LONG, T. A., TSUKAGOSHI, H., BUSCH, W., LAHNER, B., SALT, D. E. & BENFEY, P. N. 2010. The bHLH Transcription Factor POPEYE Regulates Response to Iron Deficiency in Arabidopsis Roots. *The Plant Cell,* 22**,** 2219-2236.

LÓPEZ-MILLÁN, A. F., DUY, D. & PHILIPPAR, K. 2016. Chloroplast Iron Transport Proteins – Function and Impact on Plant Physiology. *Frontiers in Plant Science,* 7**,** 178.

MCINTURF, S.A., KHAN, M.A., GOKUL, A., CASTRO-GUERRERO, N.A., HOEHNER, R., LI, J., MARGAULT, H., FICHMAN, Y., KUNZ, H.H., GOGGIN, F.L., KEYSTER, M., NECHUSHTAI, R., MITTLER, R., MENDOZA-CÓZATL, D.G. 2021 Cadmium interference with iron sensing reveals

transcriptional programs sensitive and insensitive to reactive oxygen species. *Journal of Experimental Botany* (*in press*) Sep 9:erab393. doi: 10.1093/jxb/erab393.
MENDOZA-CÓZATL, D. G., GOKUL, A., CARELSE, M. F., JOBE, T. O., LONG, T. A. & KEYSTER, M. 2019. Keep talking: crosstalk between iron and sulfur networks fine-tunes growth and development to promote survival under iron limitation. *Journal of Experimental Botany,* 70**,** 4197-4210.
MENDOZA-CÓZATL, D. G., XIE, Q., AKMAKJIAN, G. Z., JOBE, T. O., PATEL, A., STACEY, M. G., SONG, L., DEMOIN, D. W., JURISSON, S. S., STACEY, G. & SCHROEDER, J. I. 2014. OPT3 Is a Component of the Iron-Signaling Network between Leaves and Roots and Misregulation of OPT3 Leads to an Over-Accumulation of Cadmium in Seeds. *Molecular Plant,* 7**,** 1455-1469.
MUSTROPH, A., ZANETTI, M. E., JANG, C. J. H., HOLTAN, H. E., REPETTI, P. P., GALBRAITH, D. W., GIRKE, T. & BAILEY-SERRES, J. 2009. Profiling translatomes of discrete cell populations resolves altered cellular priorities during hypoxia in Arabidopsis. *Proceedings of the National Academy of Sciences of the United States of America,* 106**,** 18843-18848.
NELSON, B. K., CAI, X. & NEBENFÜHR, A. 2007. A multicolored set of in vivo organelle markers for co-localization studies in Arabidopsis and other plants. *The Plant Journal,* 51**,** 1126-1136.
NGUYEN, N. T., MCINTURF, S. A. & MENDOZA-CÓZATL, D. G. 2016. Hydroponics: A Versatile System to Study Nutrient Allocation and Plant Responses to Nutrient Availability and Exposure to Toxic Elements. *Journal of Visualized Experiments : JoVE***,** 54317.
ROBE, K., CONEJERO, G., GAO, F., LEFEBVRE-LEGENDRE, L., SYLVESTRE-GONON, E., ROFIDAL, V., HEM, S., ROUHIER, N., BARBERON, M., HECKER, A., GAYMARD, F., IZQUIERDO, E. & DUBOS, C. 2021. Coumarin accumulation and trafficking in Arabidopsis thaliana: a complex and dynamic process. *New Phytol,* 229**,** 2062-2079.
ROBINSON, N. J., PROCTER, C. M., CONNOLLY, E. L. & GUERINOT, M. L. 1999. A ferric-chelate reductase for iron uptake from soils. *Nature,* 397.
RODRÍGUEZ-CELMA, J., CHOU, H., KOBAYASHI, T., LONG, T.A., BALK, J. 2019. Hemerythrin E3 Ubiquitin Ligases as Negative Regulators of Iron Homeostasis in Plants. Frontiers in Plant Science. 10:98. doi: 10.3389/fpls.2019.00098. eCollection 2019.
ROMERA, F. J., ALCÁNTARA, E. & DE LA GUARDIA, M. D. 1992. Role of roots and shoots in the regulation of the Fe efficiency responses in sunflower and cucumber. *Physiologia Plantarum,* 85**,** 141-146.
ROSENKRANZ, T., OBURGER, E., BAUNE, M., WEBER, G. & PUSCHENREITER, M. 2021. Root exudation of coumarins from soil-grown Arabidopsis thaliana in response to iron deficiency. *Rhizosphere,* 17**,** 100296.
SANTI, S. & SCHMIDT, W. 2009. Dissecting iron deficiency-induced proton extrusion in Arabidopsis roots. *New Phytologist,* 183**,** 1072-1084.
SCHIESTL, R. H. & GIETZ, R. D. 1989. High efficiency transformation of intact yeast cells using single stranded nucleic acids as a carrier. *Current Genetics,* 16**,** 339-346.
SCHULER, M., KELLER, A., BACKES, C., PHILIPPAR, K., LENHOF, H.-P. & BAUER, P. 2011. Transcriptome analysis by GeneTrail revealed regulation of functional categories in response to alterations of iron homeostasis in Arabidopsis thaliana. *BMC Plant Biology,* 11**,** 87.
SCHULER, M., RELLAN-ÁLVAREZ, R., FINK-STRAUBE, C., ABADÍA, J. & BAUER, P. 2012. Nicotianamine functions in the Phloem-based transport of iron to sink organs, in pollen development and pollen tube growth in Arabidopsis. *The Plant cell,* 24**,** 2380-2400.
SELOTE, D., SAMIRA, R., MATTHIADIS, A., GILLIKIN, J. W. & LONG, T. A. 2015. Iron-binding E3 ligase mediates iron response in plants by targeting basic helix-loop-helix transcription factors. *Plant physiology,* 167**,** 273-286.
SIVITZ, A. B., HERMAND, V., CURIE, C. & VERT, G. 2012. Arabidopsis bHLH100 and bHLH101 control iron homeostasis via a FIT-independent pathway. *PloS one,* 7**,** e44843-e44843.
VAROTTO, C., MAIWALD, D., PESARESI, P., JAHNS, P., SALAMINI, F. & LEISTER, D. 2002. The metal ion transporter IRT1 is necessary for iron homeostasis and efficient photosynthesis in Arabidopsis thaliana. *The Plant Journal,* 31.
VERT, G., GROTZ, N., DÉDALDÉCHAMP, F., GAYMARD, F., GUERINOT, M. L., BRIAT, J.-F. & CURIE, C. 2002. IRT1, an Arabidopsis Transporter Essential for Iron Uptake from the Soil and for Plant Growth. *The Plant Cell,* 14**,** 1223-1233.
VERT, G. A., BRIAT, J. F. & CURIE, C. 2003. Dual regulation of the Arabidopsis high-affinity root iron uptake system by local and long-distance signals. *Plant Physiol,* 132.
WATERS, B. M., CHU, H.-H., DIDONATO, R. J., ROBERTS, L. A., EISLEY, R. B., LAHNER, B., SALT, D. E. & WALKER, E. L. 2006. Mutations in Arabidopsis Yellow Stripe-Like1 and Yellow Stripe-Like3 Reveal

Their Roles in Metal Ion Homeostasis and Loading of Metal Ions in Seeds. *Plant Physiology,* 141**,** 1446-1458.
WINTZ, H., FOX, T., WU, Y.-Y., FENG, V., CHEN, W., CHANG, H.-S., ZHU, T. & VULPE, C. 2003. Expression Profiles of Arabidopsis thaliana in Mineral Deficiencies Reveal Novel Transporters Involved in Metal Homeostasis. *Journal of Biological Chemistry,* 278**,** 47644-47653.
WYDRO, M., KOZUBEK, E. & LEHMANN, P. 2006. *Optimization of transient Agrobacterium-mediated gene expression system in leaves of Nicotiana benthamiana*.
YUAN, Y., WU, H., WANG, N., LI, J., ZHAO, W., DU, J., WANG, D. & LING, H. Q. 2008. FIT interacts with AtbHLH38 and AtbHLH39 in regulating iron uptake gene expression for iron homeostasis in Arabidopsis. *Cell Res,* 18.
ZHAI, Z., GAYOMBA, S. R., JUNG, H.-I., VIMALAKUMARI, N. K., PIÑEROS, M., CRAFT, E., RUTZKE, M. A., DANKU, J., LAHNER, B., PUNSHON, T., GUERINOT, M. L., SALT, D. E., KOCHIAN, L. V. & VATAMANIUK, O. K. 2014. OPT3 Is a Phloem-Specific Iron Transporter That Is Essential for Systemic Iron Signaling and Redistribution of Iron and Cadmium in Arabidopsis. *The Plant Cell Online*.
ZHANG, C. 2014. Essential functions of iron-requiring proteins in DNA replication, repair and cell cycle control. *Protein & cell,* 5**,** 750-760.
ZHANG, J., LIU, B., LI, M., FENG, D., JIN, H., WANG, P., LIU, J., XIONG, F., WANG, J. & WANG, H.-B. 2015. The bHLH Transcription Factor bHLH104 Interacts with IAA-LEUCINE RESISTANT3 and Modulates Iron Homeostasis in Arabidopsis. *The Plant Cell,* 27**,** 787-805.
ZIEGLER, J., SCHMIDT, S., STREHMEL, N., SCHEEL, D. & ABEL, S. 2017. Arabidopsis Transporter ABCG37/PDR9 contributes primarily highly oxygenated Coumarins to Root Exudation. *Scientific Reports,* 7**,** 3704.

Figure legends

Figure 1. AtZIP5 is capable of mobilizing iron in yeast. **(A)** Growth of *fet3 fet4* yeast expressing At*ZIP5* on medium without Fe and **(B)** Fe accumulation in yeast cells expressing At*ZIP5 or AtIRT1* (n = 4 yeast cultures, mean ± S.E.); asterisks indicate a significant difference with a p-value < 0.05. Statistical analysis One-way ANOVA and Turkey pairwise comparison tests were performed using the Minitab statistical package.

Figure 2. **AtZIP5 is preferentially expressed in the vasculature and localized to the plasma membrane**. **(A-B)** GUS staining of *ZIP5p::GUS* leaves indicate that AtZIP5 expression localizes to the vasculature tissue. (**C-E)** Transient expression of *YFP*-At*ZIP5* under the control of *CaMV 35S* promoter in tobacco cells co-infiltrated with the plasma membrane maker PIP2A-mCherry, three-day post infiltration. **(E)** Overlay image shows AtZIP5 localized to the plasma membrane of the cells. **(C)** mCherry channel, **(D)** YFP channel, **(E)** overlay of C and D, (**F**) Fluorescence intensity plot showing two peaks corresponding to the 2 plasma membranes of neighboring cells. Overlapping peaks in the two channels indicate colocalization of YFP-ZIP5 with the plasma membrane marker PIP2A-mCherry.

Figure 3. **Overexpression of AtZIP5 in companion cells promotes increased sensitivity to Fe limitation (A)** 10 day-old seedlings of *ZIP5ox 16-10* and *ZIP5ox 25-5* showed shorter roots compared to WT when grown in Fe deficient media (+Fe, 50 µM Fe-EDTA; Fe, no Fe with 0.15 mM of ferrozine). **(B)** Quantification of root growth of *ZIP5ox* plants grown on Fe deficiency plates (n = 6- 10 plants; mean ± S.E.). Experiment was repeated three times with similar results. Asterisks indicate a significant difference with a p-value < 0.05.

Figure 4. Altered Fe deficiency responses in *ZIP5ox* lines. **(A-C)** Relative expression Fe deficiency markers in ZIP5ox lines compared to wildtype . **(D)** Relative expression of root-specific makers for Fe deficiency responses. 4-week-old plants (12 days grown on one-quarter MS medium plates and 18 days grown on hydroponics under Fe

sufficient condition, 50 µM Fe-EDTA) were transferred hydroponic media and at the indicated times young leaves, mature leaves, and roots were collected separately for further processing. Data represent three independent experiments, each with three biological replicates. Data show mean ± SE, asterisks indicate significant difference with a p-value < 0.05. T-tests were performed using the Minitab statistical package.

Figure 5. Fe precipitation in the leaf vasculature of *nas4x-1* results in reduced shoot-to-root Fe transport. (A) Synchrotron X-ray imaging shows that mature leaves of *nas4x-1* had a higher signal of Fe around the vasculature compared to Col-0 and *ZIP5ox* lines. (**B**) Pixel intensity of XRF images extracted with the 3D surface plot package of Image J shows consistent lower Fe signal in *ZIP5ox* lines. **(C)** The lower Fe signal in ZIP5ox lines is more evident in the veins near the edge of the leaf. **(D)** Leaf-to-root transport assay of radioactive ^{59}Fe indicated that *nas4x-1* transported less Fe downward the roots under Fe sufficient condition. Data show mean ± SE of 5 biological replicates. Asterisks indicate a significant difference with a p-value < 0.05. T-tests were performed using the Minitab statistical package.

Figure 6. ***nas4x-1* exhibits a constitutive Fe deficiency responses in sink tissues. (A-C)** Relative expression of Fe deficiency markers in *nas4x-1* **(D)** Relative expression of root specific Fe deficiency makers in *nas4x-1*. Plant growth conditions and tissue collection were described in Figure 4 and methods section. Data represent three independent experiments, each with three biological replicates. Data show mean ± SE; asterisks indicate significant difference with a p-value < 0.05. T-tests were performed using the Minitab statistical.

Figure 1

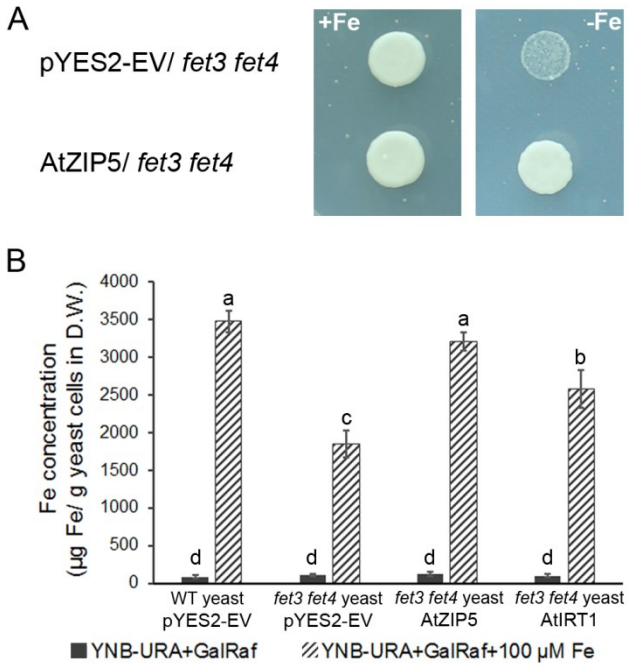

Figure 2

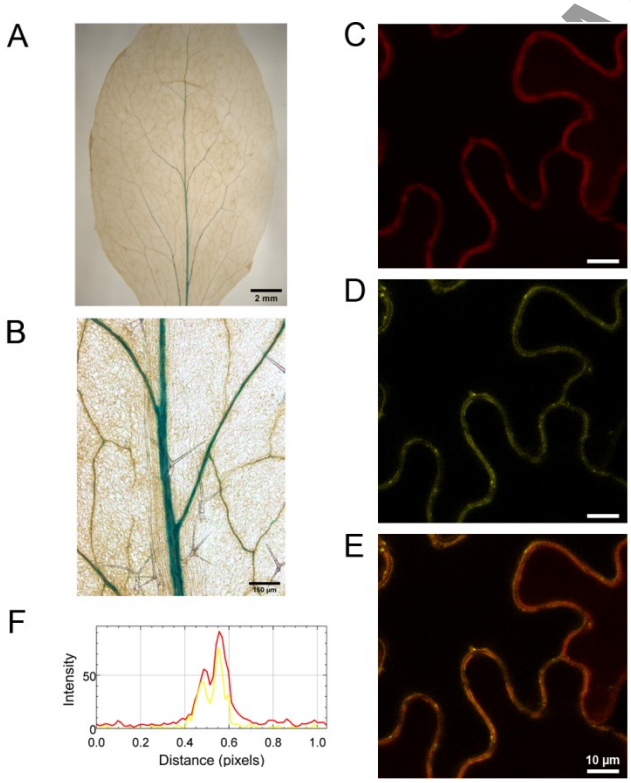

Figure 3

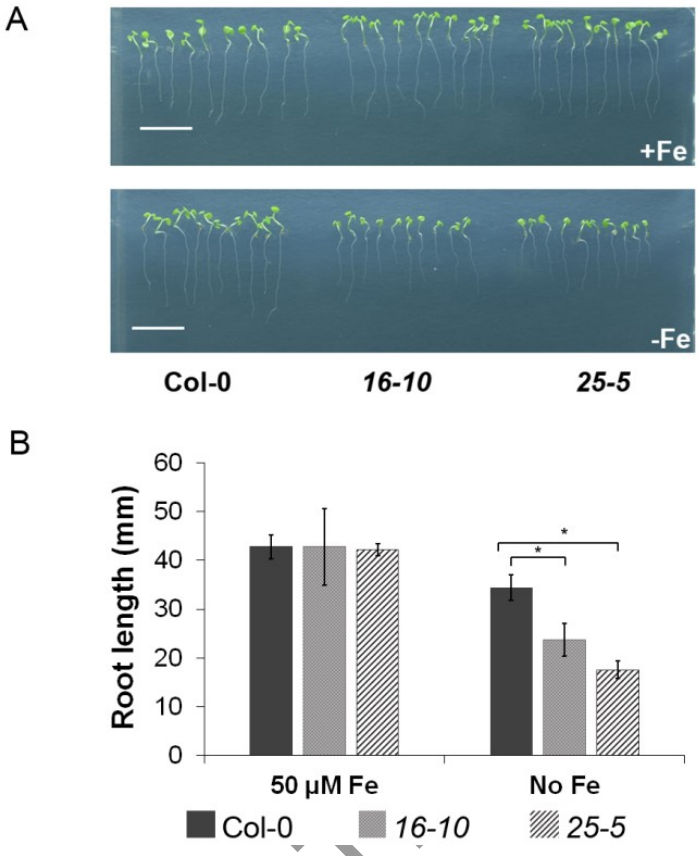

Figure 4

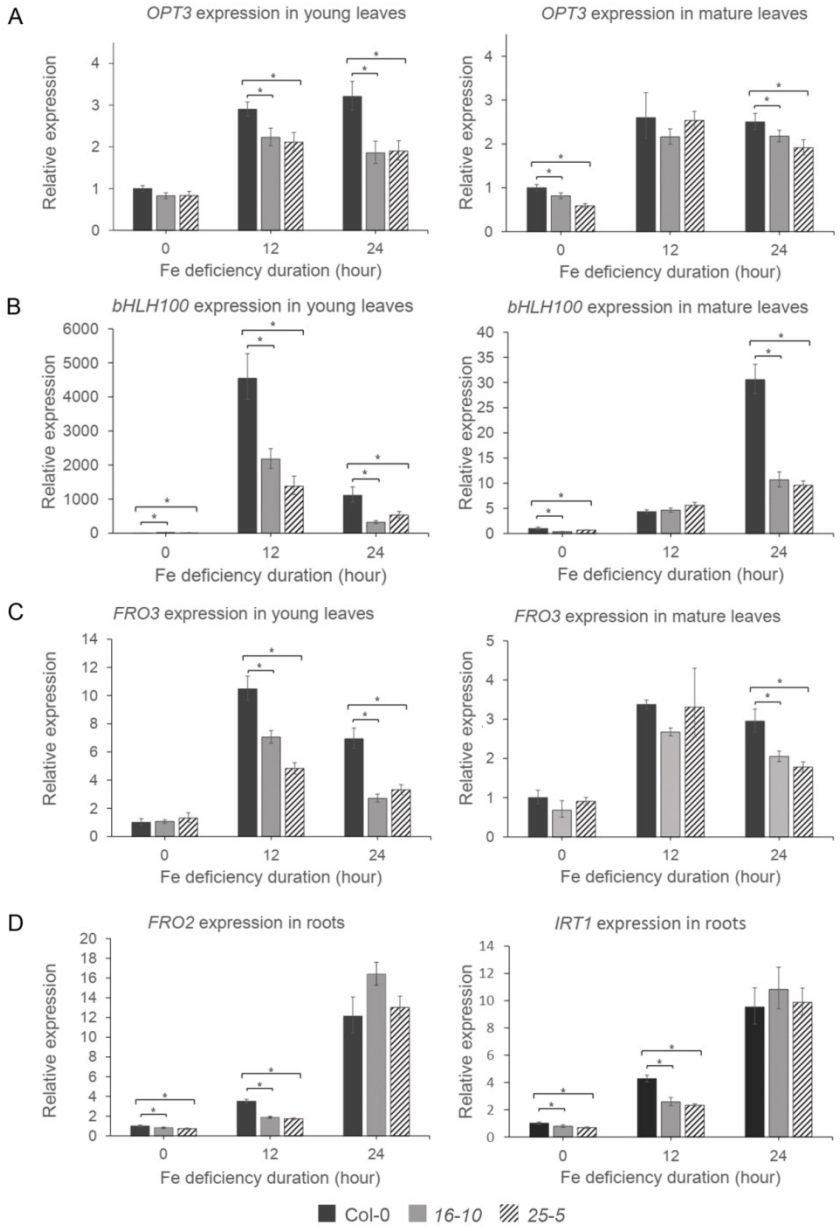

Figure 5

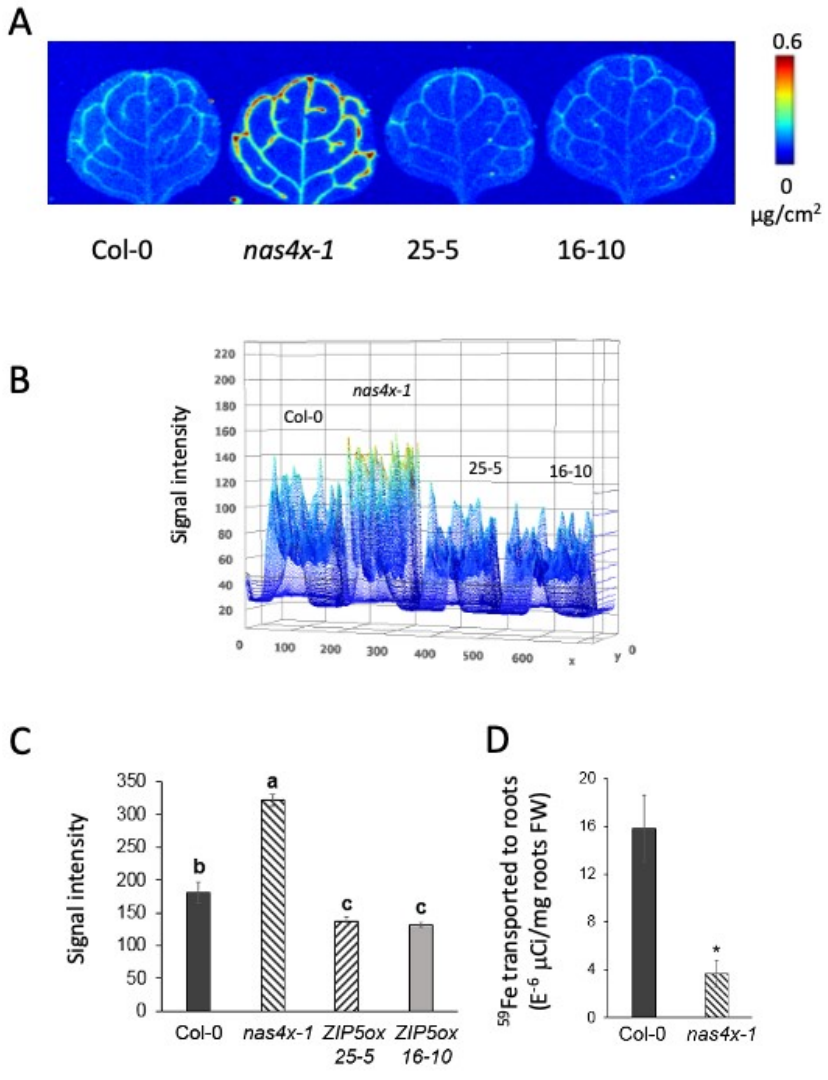

Figure 6